Cascade Control of a Residual Water Blunting System

Vlad MUREŞAN, Mihail ABRUDEAN, Mihaela-Ligia UNGUREŞAN, Tiberiu COLOŞI
Technical University of Cluj-Napoca, Automation Department, 26-28 Gh. Barițiu Street, 400027, Cluj-Napoca, Romania
Vlad.Muresan@aut.utcluj.ro,Mihai.Abrudean@aut.utcluj.ro,Mihaela.Unguresan@chem.utcluj.ro, Tiberiu.Colosi@aut.utcluj.ro

***Abstract*—In this paper, a solution for the automatic control of a residual water blunting system is proposed. The blunting technological process, being a distributed parameter one, is modeled using partial differential equations. This approach implies very big technological advantages due to the fact that the user has access to the pH value in each point of the tanks of the blunting system. Another element of originality is the inclusion of a distributed parameter process in a control structure, having the possibility to maintain the pH value constant in each point in the volume of the liquid from the system. A method based on the matrix of partial derivatives of the state vector (Mpdx) associated with Taylor series is used for the modeling-simulation of both the blunting process and the control system. The results assured by a simple control structure are not sufficient due to the restrictive imposed performances, so a cascade structure is treated in the paper.**

***Index Terms*—automatic control, control system, distributed parameter process, numerical simulation, partial differential equation.**

I. Introduction

The blunting system treated in this paper has the purpose to assure a pH value very close to 7 (the indifferent pH value) [1] of the residual water that results from different points of the technological flow of producing seamless steel pipes. The accuracy of the pH automatic control has to be a very high one because the minimum (6.5) and maximum (7.5) limits (imposed by law) must not be reached at the overflowing point from the system. Only if these constrains are respected, the ecosystem (in general the closest valley) where the residual water is overflowed is protected against pollution [2].

In its structure the blunting system contains four consecutive (in relation to their length) neutralizing tanks. Taking in consideration that in this application the residual water has an acid character, the used neutralizer is the cream of lime, a basic solution having pH equal to 12. The input point in the system is the edge (in relation to its length) of the first tank, where both substances are introduced in the reaction through the corresponding pipes (the edge that does not communicate with the second tank). Also, the output point from the system corresponds to the overflowing point of the last tank (tank four), being the edge that does not communicate with tank number three. The circulation between the input and output points appears due to the difference of level between each consecutive tanks, due to the fact that the substances are introduced continuously in the tanks and due to the fact that each tank is equipped with a barbotage system (system that assures the chemical homogenization, too).

Considering the fact that the set of performances imposed on the control system is very restrictive, a simple control structure with an on-off controller or with only one PID controller is not sufficient to be used. The pH variation is very high especially in the first tank, fact that introduces the premise of using a cascade control system. In this context, the first tank will be considered the first blunting subsystem, with the main property that the pH variation is very fast in it.

Using this approach, the effect of the main disturbance (the acid that is introduced in the reaction) can be rejected very efficiently in this tank. The second blunting subsystem will be an equivalent tank that can replace the other three tanks of the system. The equivalent tank can be considered in this case because the three tanks have the same technical characteristics and the same technological functions.

Both the technical characteristics of the tank number 1 associated to the first subsystem and those of the equivalent tank associated to second one, are presented in the Table I:

TABLE I. TECHNICAL CHARACTERISTICS OF THE TANKS

Technical characteristics of the tank	**Length**	**Width**	**Depth**	**Volume**
Tank 1	5 m	2 m	1.5 m	15 m^3
Equivalent Tank (Tank 2 + Tank 3 + Tank 4)	15 m	2 m	1.5 m	45 m^3

The general diagram of the blunting system, decomposed in two sub-systems, is presented in Fig. 1.

From Fig. 1, we can remark that the pH transducers are installed at the overflowing point of the two tanks, assuring the feedback signals (in unified current) for the two pH controllers AC1 and AC2. The two controllers are connected in cascade, AC1 generating the reference to AC2. The control signals (1 and 2) are unified current signals, too. The control signal 2 adjusts the opening grade of the electro-valve (the actuator) that assures the input of a certain flow of neutralizer in the reaction.

The back-up cream of lime pipe belongs to the equivalent tank and is used only in the fault procedures.

This control system generates very high performances in stabilizing the value of the output signal, more exactly the chemical pH value at the output of the blunting system (the output of the equivalent tank).

Digital Object Identifier 10.4316/AECE.2014.02022

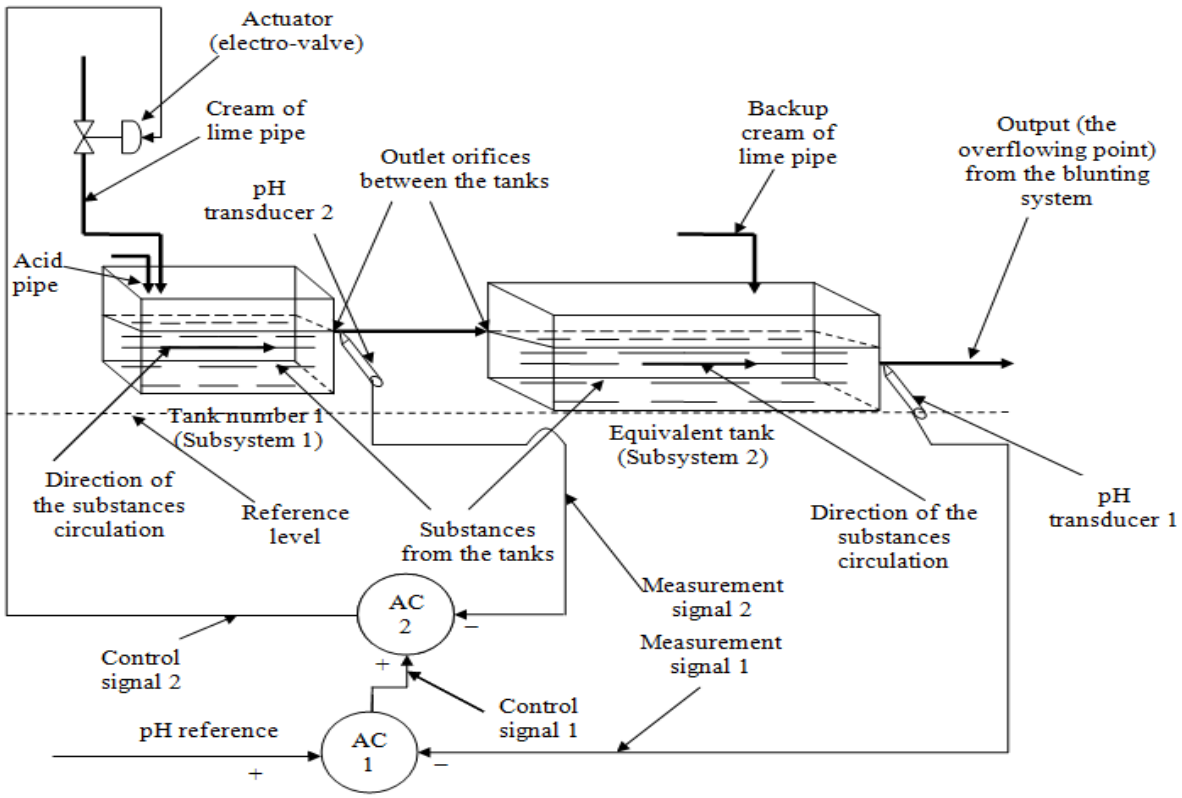

Figure 1. The general diagram of the blunting system

II. The Mathematical Model of the Blunting Process

The pH variation of the chemical from the blunting system varies, obviously, in relation to the independent variable time (t). But besides that, the pH variation appears, too, due to the fact that the reaction between the two reactants occurs progressively from the input point in each tank to the overflowing point of each tank (phenomenon that is determined by the chemical circulation in the tanks).

Considering this aspect, other independent variables that determine the position in each tank can be introduced in the model of the process.

In this case the residual water blunting process (system) is treated as a distributed parameter one.

The independent variables associated to the position in the system are introduced using the Cartesian space representation, as it can be remarked in the following figure (Fig. 2).

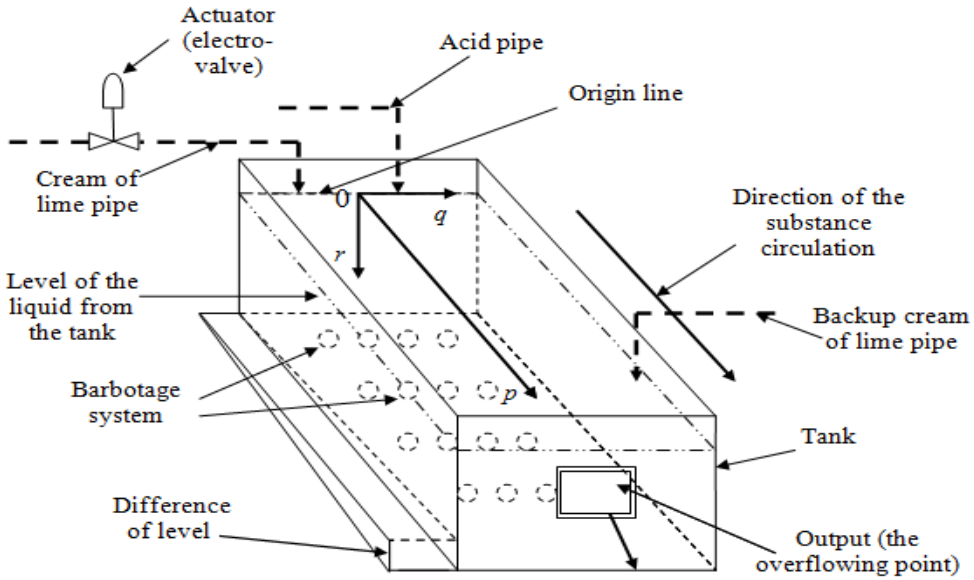

Figure 2. The general structure of the tank associated to one from the two subsystems

In Fig. 2 the general structure of the two tanks from Fig. 1 is presented.

The two input pipes (for cream of lime and acid) represented with dashed line are used only in the case of tank number 1. The backup cream of lime pipe and the difference of level represented with dashed line too, are marked only in the case of the equivalent tank. The difference of level between the input and the overflowing point (a small one) in the case of the equivalent tank compensates the level difference between the three

consecutive tanks that are viewed as an equivalent one. The following approach is valid for both cases.

The pH variation on the tank's length, width and depth corresponds to the pH variation on the 0*p*, 0*q*, respectively 0*r* axes. The pH's value homogenization is made with a very high efficiency especially in the tank's width, respectively depth due to the barbotage system. This aspect implies the fact that the pH variation on the 0*q* and 0*r* axes has an insignificant weight comparing to the pH variation on the 0*p* axis case. Considering the previous remark, the conclusion is that in the model of the blunting process, only the pH variation on the 0*p* axis is considered. In other words, besides the time independent variable (*t*), only the "length" independent variable (*p*) is considered.

The model of distributed parameter processes [3-9] can be expressed using partial differential equations (PDE). The general partial differential equation that describes how the two processes work (associated to the two blunting subsystems) is of second order with two independent variables (time and length) (PDE II·2). The mentioned general equation is presented in (1), being considered the notation: $y_{TP} = \frac{\partial^{T+P} y}{\partial t^T \partial p^P}$, where *T*=0,1,2…., and *P*=0,1,2,.. .

$$a_{00} \cdot y_{00} + a_{10} \cdot y_{10} + a_{01} \cdot y_{01} + a_{20} \cdot y_{20} + \\ + a_{11} \cdot y_{11} + a_{02} \cdot y_{02} = \varphi_{00} \quad . \tag{1}$$

In (1) the coefficients are constant and the functions $y(t, p)$ (the pH value of the chemical from the tank) and $\varphi(t, p)$ respect Cauchy conditions of continuity. The notation associated to the differentiation order used in the case of y function, is valid for φ function, too.

The modeling procedure is the same for both blunting subsystems with the difference that the input signals in the second subsystem are the output signals of the first subsystem. To obtain the model of processes, the input flow of the two reacting substances will be considered constant. The previous remark implies the fact that the output signals of the processes result from the pH value of the reacting substances at the input point in the corresponding tank.

At the initial moment the assumption that the two tanks are full with liquid with pH value equal to 7 is made and the concentration of the liquid is homogenous in the tanks volume.

Next, the modeling procedure for tank number 1 is presented.

Due to the fact that two reacting substances are introduced in the tank, the blunting process associated to the first tank can be decomposed in two sub-processes connected in parallel. In the first sub-process case, the acid is introduced in the tank and in the same time, through the cream of lime pipe, a liquid with the pH value equal to 7 is introduced. The input signal has the value equal to the difference between the acid's pH and 7. Hence, the input signal $u_A(t)$ will have a negative step variation form. The effect of applying this signal at the input of the sub-process is a decreasing evolution of the value of the output signal $y_{AI}(t, p)$ under the value of 7 (pH indifferent value from the chemical point of view). In the second sub-process case, the cream of lime is introduced in the tank and in the same time, through the acid pipe, a liquid with the pH value equal to 7 is introduced. The input signal $u_B(t)$ has the value equal to the difference between the cream of lime's pH and 7. Hence, the input signal will have a positive step variation form. The effect of applying the positive step signal at the input of the second sub-process is an increasing evolution of the value of the output signal $y_{BI}(t, p)$ over the value of 7. The model of each sub-process can be expressed using the equation from relation (1) by replacing y function with $y_{AI}(t, p)$ or $y_{BI}(t, p)$. The output signal of the blunting process associated to the first tank will be the sum between the output signals from the two sub-processes:

$$y_I(t, p) = y_{AI}(t, p) + y_{BI}(t, p) . \tag{2}$$

The $y_I(t, p)$ signal represents the pH value of the chemical from the first tank if both the acid and the cream of lime are introduced through the corresponding pipes.

For the equivalent tank, the procedure is the same, but the input signals are considered $y_{AI}(t, p)$ and $y_{BI}(t, p)$ instead of $u_A(t)$ and $u_B(t)$. Also the notations for the two sub-processes output signals are $y_{AF}(t, p)$, respectively $y_{BF}(t, p)$ and the output signal from the process is:

$$y_F(t, p) = y_{AF}(t, p) + y_{BF}(t, p) . \tag{3}$$

In Fig. 3, the block diagram of the blunting process is presented. The sub-processes are numbered from 1 to 4 as it can be noticed in the figure.

Due to the fact that the two tanks are connected in series and the processes associated to the tanks can be decomposed each in two sub-processes, it results (Fig. 3) a combined serial and parallel connection of four PDEs. Only a subscript attached to the function $u_{0A}(t)$, respectively $u_{0B}(t)$ (without considering the A and B letters that determine the sub-process) signifies the differentiation order of those elements related to independent variable (*t*). This notation remains valid for the following intermediary signals presented in this paper, too. The approximating analytical solutions that verify relation (1), for the four sub-processes are:

$$y_{00ANi}(t, p) = K_y \cdot F_{0Ti}(t) \cdot F_{0Pi}(p) \cdot u_{0i}(t) \tag{4}$$

where *i* can be A1, A2, B1 or B2. In relation (4) K_y represents the proportionality constant of the process. K_y is a dimensionless coefficient and after some analytical calculations results $K_y = 0.25$. Also

$F_{0Ti}(t) = 1 - \frac{T_1}{T_1 - T_2} \cdot e^{-\frac{t}{T_1}} - \frac{T_2}{T_2 - T_1} \cdot e^{-\frac{t}{T_2}}$, and

$F_{0Pi}(p) = \sigma_0 + \sigma_1 \cdot e^{-\frac{p}{P_1}} + \sigma_2 \cdot e^{-\frac{p}{P_2}}$. T_1 and T_2 are the time constants of the process respectively P_1 and P_2 can be called "the length constants" of the process. σ coefficients will be detailed later in this chapter.

After accomplishing the necessary experiments on the plant, it results that the speed of the chemical reaction decreases with the length increasing on the 0*p* axis.

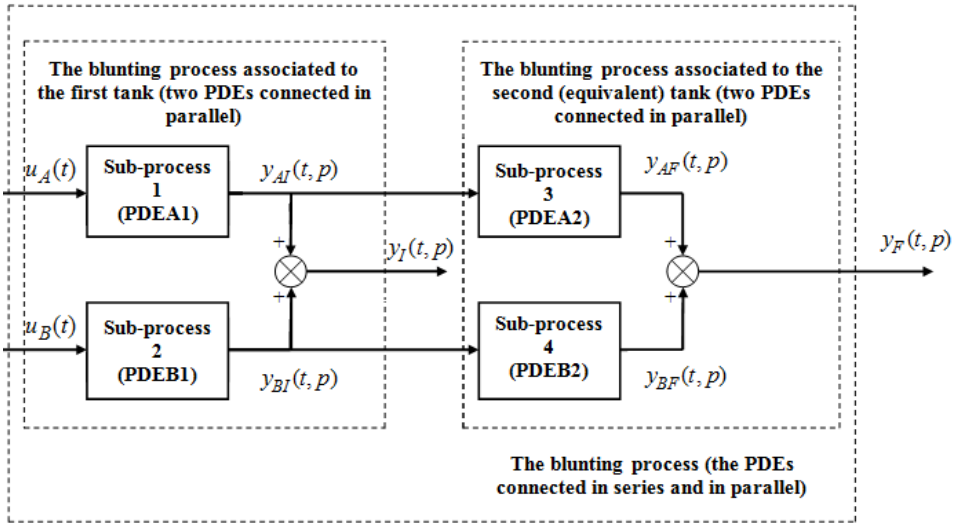

Figure 3. The block diagram of the blunting process

The effect of this remark is that the value of the time constants T_1 and T_2 differs for different points on the $0p$ axis.

Hence, higher the value of the distance from the origin of the Cartesian system on the $0p$ axis is, higher the values of the time constants are.

The evolution of the analytical solution of the equation from relation (1) singularized for the sub-processes A1 and A2, related to the two independent variables (t and p), $u_A(t)$ being a negative step signal, is qualitatively presented in Fig. 4.

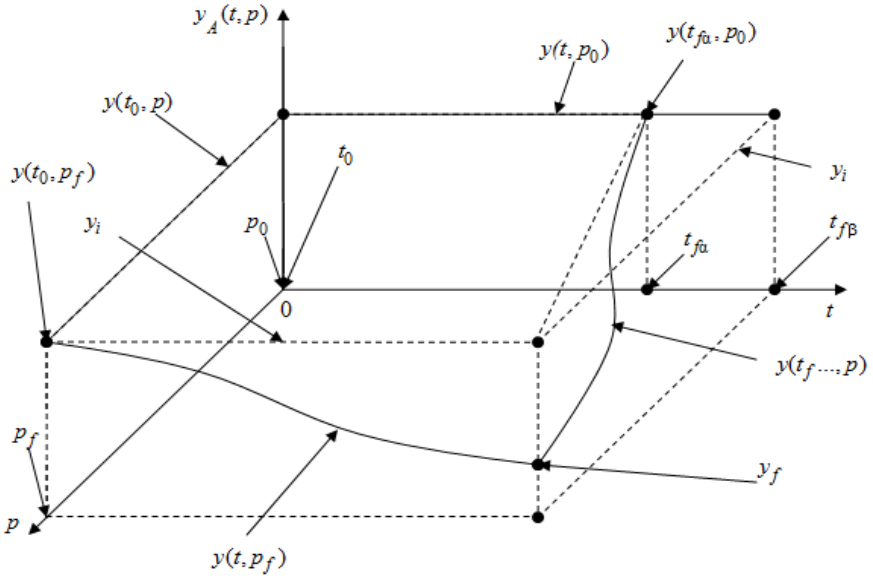

Figure 4. The evolution of the analytical solution related to t and p, for the sub-processes A1 and A2

Also, the evolution of the analytical solution of the equation from relation (1) singularized for the sub-processes B1 and B2, related to the two independent variables (t and p), $u_B(t)$ being a positive step signal, is qualitatively presented in Fig. 5.

The analytical model was approximated using some intermediary representative measurements from the process. In Figs. 4 and 5, the indices 0 signify the initial values, i indices signify the initial values, f indices signify the final values, respectively indices α and β signify the difference between the settling time of the response for p_0 and for p_f.

On the origin line, the reaction does not occur, the value of the response remaining constant at the value 7 (y_i). In the immediate neighborhood of the origin (p_0), the reaction occurs very fast but the pH value (for $t_{f\alpha}$) remains near 7 (y_i) because the reaction is only at the start. At the overflowing point (p_f) the reaction appears slower but the pH value (for $t_{f\beta}$) presents a maximum variation in relation to (y_i) because the reaction is complete.

From Fig. 4 and Fig. 5, results the antagonistic effect of the acid, respectively of the cream of lime introduced in the process. Making the sum of the two effects and considering the appropriate values of the flows of the two substances, the resultant will become null creating the possibility to control [10-12] the pH value.

The experimental identification is applied in order to obtain the structure parameters of the process, more exactly the time constants and the “length constants” of the process.

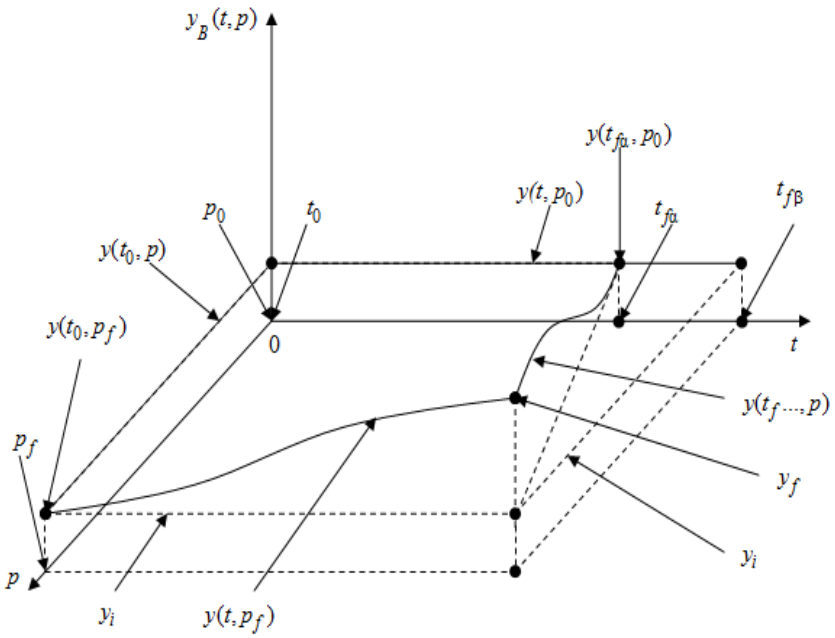

Figure 5. The evolution of the analytical solution related to t and p, for the sub-processes B1 and B2

The experiment is based on the step response of the blunting process. The experimental curves are obtained measuring the evolution in time of the pH value in different points located on the lengths of the tanks of the system (including the input point in the system, some intermediary points and the overflowing point of the system).

The time constants are identified using the tangent method [13,14], resulting the values $T_{1\alpha} = 2.56\,\text{min}$ and $T_{2\alpha} = 3.84\,\text{min}$ for $y(t, p_0)$, respectively $T_{1\beta} = 7.04\,\text{min}$ and $T_{2\beta} = 10.56\,\text{min}$ for $y(t, p_f)$. The evolution of the time constants from p_0 to p_f is approximately linear and is given by relations: $T_{1\gamma} = T_{1\alpha} + \frac{T_{1\beta} - T_{1\alpha}}{p_f - p_0} \cdot p$, $T_{2\gamma} = T_{2\alpha} + \frac{T_{2\beta} - T_{2\alpha}}{p_f - p_0} \cdot p$ where $p_0 \le p \le p_f$ and $t_\alpha \le t_\gamma \le t_\beta$.

"The length constants" of the process are identified using a method based on an interpolation procedure, resulting the values $P_1 = 1.6\,\text{m}$ and $P_2 = 2.4\,\text{m}$. Using these values, the *a*... coefficients from relation (1) can be calculated with the next formulae: $a_{00} = 1$, $a_{10} = T_{1\gamma} + T_{2\gamma}$, $a_{20} = T_{1\gamma} \cdot T_{2\gamma}$, $a_{01} = P_1 + P_2$, $a_{02} = P_1 \cdot P_2$ and $a_{11} = (T_{1\gamma} + T_{2\gamma}) \cdot (P_1 + P_2)$. Also σ coefficients from the relations of $F_{0Pi}(p)$ can be calculated with the following formulae: $\sigma_{0i} = \frac{y_{fi}}{u_{0i}}$, $\sigma_{1i} = \frac{y(t_{f\alpha i}, p_0) - y_{fi}}{u_{0i}} \cdot \frac{P_1}{P_1 - P_2}$, respectively $\sigma_{2i} = \frac{y(t_{f\alpha i}, p_0) - y_{fi}}{u_{0i}} \cdot \frac{P_2}{P_2 - P_1}$ where $i \in \{A1, A2, B1, B2\}$.

The identified time and length constants, being structure parameters, remain the same for all four sub-processes.

III. Mathematical Modeling and Numerical Simulation of the Control Structure

The cascade control structure [15] is presented in Fig. 6.

In Fig. 6, the internal loop is associated to the first tank of the blunting system. Its output signals $y_{AI}(t,p)$, $y_{BI}(t,p)$ and implicitly their sum $y_I(t,p)$ have a much faster variation comparing to the corresponding signals from the external loop ($y_{AF}(t,p)$, $y_{BF}(t,p)$ and $y_F(t,p)$).

The process associated to the equivalent tank is placed in the external loop. The output signals from the internal loop are input signals for the external one. The faster variation of the signals from the internal loop comparing to the signals from the external one is given by the fact that the length of tank number one is three times smaller than the length of the equivalent tank (the time constants value depending on the length as it was determined in the previous chapter) and due to the fact that the input signals in the blunting system correspond to the input signals in the first tank. The measured signals are $y_I(t,p)$, respectively $y_F(t,p)$.

The significance of the new notations from Fig. 6 is: C_1–main PID controller (associated to the external loop); C_2–secondary PID controller (associated to the internal loop); A–actuator (the electro-valve); MT1, MT2–pH transducers; $af(t) = af_0$–main error signal; $ai(t) = ai_0$ –secondary error signal; $cf(t) = cf_0$–control signal generated by C_1; $ci(t) = ci_0$–control signal generated by C_2; $w(t) = w_0$–reference signal; $f(t) = f_0$–actuating signal representing the flow of the cream of lime, after the actuations generated by controllers; $mI(t) = m_{I0}$, $mF(t) = mF_0$–measurement signals. K_{pH} represents a proportionality constant equal to 5 (pH of cream of lime–7). In the case of the control structure, $u_A(t)$ and $u_B(t)$ represent the multiplication results between the flow of the two reactants and the values of the differences between their

pH and 7. In the control structure [16-19], the effect of the acid (the outputs of PDEA1 and PDEA2) can be viewed like a disturbance signal. The analogue modeling of the system presented in Fig. 6 starts from the following system of equations:

Transducer 1:

$$\begin{cases} mI_0 \\ mI_1 = \dfrac{1}{T_T}\cdot[K_T\cdot(y_{00AI}+y_{00BI})-mI_0] \end{cases}. \quad (5)$$

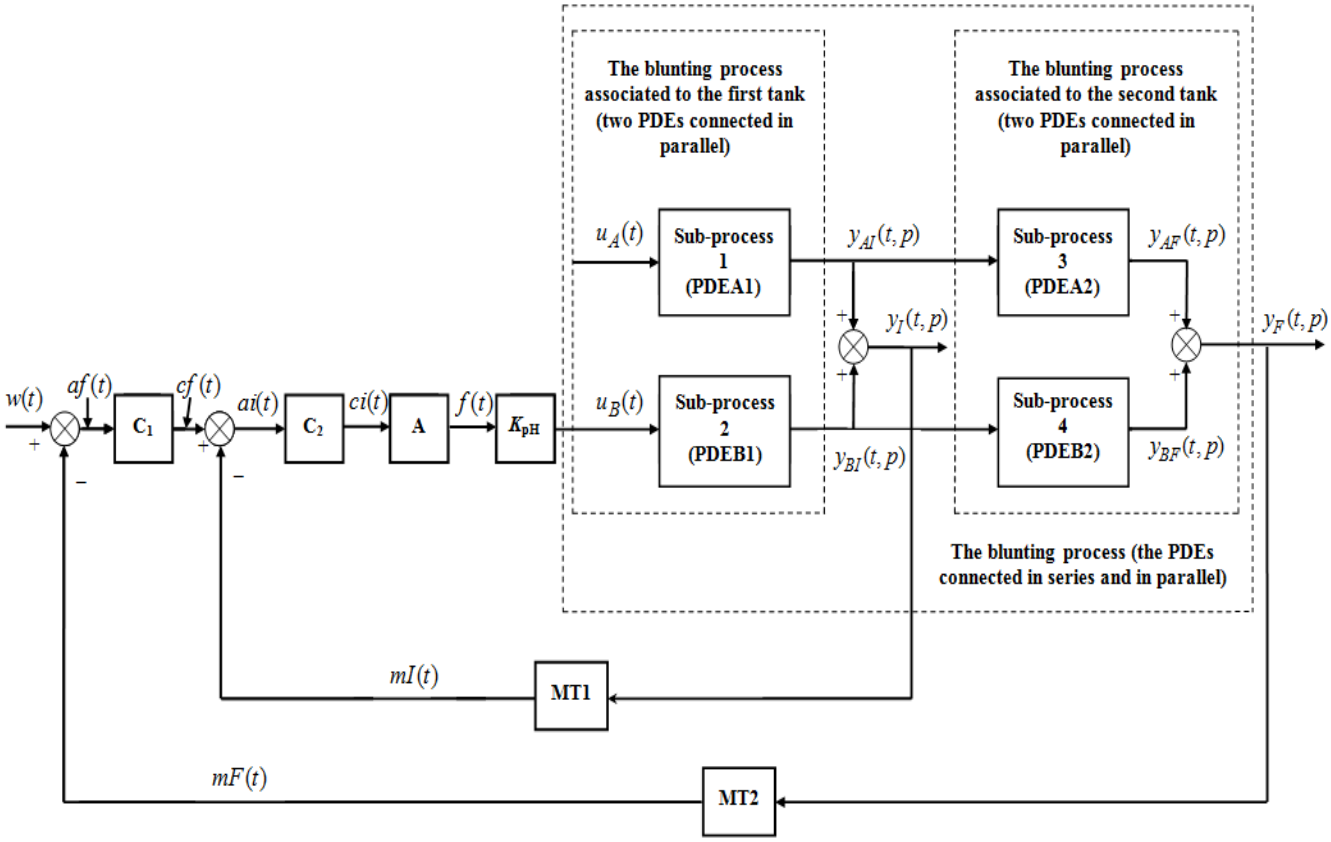

Figure 6. The cascade control structure

Transducer 2:

$$\begin{cases} mF_0 \\ mF_1 = \dfrac{1}{T_T}\cdot[K_T\cdot(y_{00AF}+y_{00BF})-mF_0] \end{cases}. \quad (6)$$

PID controller 1 (C_1):

$$\begin{cases} cf_0 \\ cf_1 = \dfrac{1}{T_R}\cdot[K_{PRF}\cdot(w_0-mF_0)+K_{DRF}\cdot(w_1-mF_1)- \\ \qquad -cf_0] \\ cf_2 = \dfrac{1}{T_R}\cdot[K_{PRF}\cdot(w_1-mF_1)+K_{IRF}\cdot(w_0-mF_0)+ \\ \qquad +K_{DRF}\cdot(w_2-mF_2)-cf_1] \end{cases}. \quad (7)$$

PID controller 2 (C2):

$$\begin{cases} ci_0 \\ ci_1 = \dfrac{1}{T_R}\cdot[K_{PRI}\cdot(w_0-mI_0)+K_{DRI}\cdot(w_1-mI_1)- \\ \qquad -ci_0] \\ ci_2 = \dfrac{1}{T_R}\cdot[K_{PRI}\cdot(w_1-mI_1)+K_{IRI}\cdot(w_0-mI_0)+ \\ \qquad +K_{DRI}\cdot(w_2-mI_2)-ci_1] \end{cases}. \quad (8)$$

Actuator:

$$\begin{cases} u_{0B} \\ u_{1B} = \dfrac{1}{T_{EE}}\cdot(K_{pH}\cdot K_{EE}\cdot ci_0-u_{0B}) \end{cases}. \quad (9)$$

Sub-processes 1-4 ($i\in$ { AI,AF,BI,BF}) (PDE II·2):

$$\begin{cases} y_{00i} \\ y_{10i} \\ y_{20i} = \dfrac{1}{a_{20}}\cdot[\varphi_{00i}-(a_{00}\cdot y_{00i}+a_{10}\cdot y_{10i}+ \\ \qquad +a_{01}\cdot y_{01i}+a_{11}\cdot y_{11i}+a_{02}\cdot y_{02i})] \end{cases}. \quad (10)$$

In the previous relations, the following symbols have also been used: K_T – proportionality constant of transducers, T_T – time constant of transducers (the two transducers are of the same type), K_{PRF} – proportionality constant of first controller (C_1), K_{IRF} – integrative constant of first controller (C_1), K_{DRF} – derivative constant of first controller (C_1), K_{PRI} – proportionality constant of second controller (C_2), K_{IRI} – integrative constant of second controller (C_2), K_{DRI} – – derivative constant of second controller (C_2), T_R –inertial time constant of each controller (both controllers are of the same type), K_{EE} –proportionality constant of actuator and

T_{EE} – time constant of actuator.

The elements of the state vector x_B associated to the control system (Fig. 7) result from the relations (5-10). Also, the elements of the state vector x_A (Fig. 7) (associated to PDEA1 and PDEA2) are obtained using the relation (10).

The two state vectors are presented in transposed form:

$$\mathbf{x_B}^T = \begin{array}{|c|c|c|c|c|c|c|c|c|c|c|c|c|c|}\hline mI_0 & mI_1 & mF_0 & mF_1 & cf_0 & cf_1 & ci_0 & ci_1 & u_{0B} & u_{1B} & y_{00BI} & y_{10BI} & y_{00BF} & y_{10BF} \\ \hline \end{array}$$

$$\mathbf{x_A}^T = \begin{array}{|c|c|c|c|}\hline y_{00AI} & y_{10AI} & y_{00AF} & y_{10AF} \\ \hline \end{array}$$

Figure 7. The x_B and x_A state vectors in the transposed form

Considering the values M=8 and N=35, respectively M=8 and N=10 that define the dimension of the matrices M_{pdxB} and M_{pdxA} (the matrix of partial derivatives of the state vector), these are presented in Fig. 8 [20].

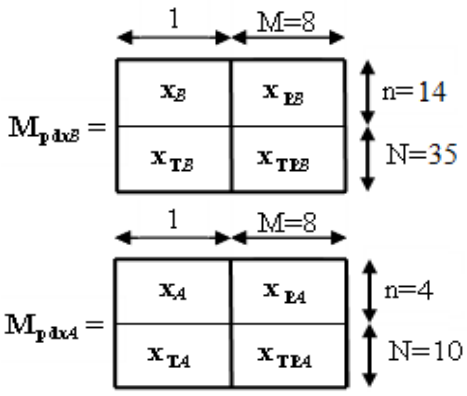

Figure 8. The M_{pdxB} and M_{pdxA} matrices

The matrices and vectors that occur in Fig. 8 are: state vector x_i; vector of partial derivatives related to time (t) of the state vector x_{Ti}; matrix of partial derivatives related to independent variable (p) of the state vector x_{Pi}; matrix of partial derivatives related to time (t) and to the independent variable (p) of the state vector x_{TPi}; i can be A or B. Thus, it results that the matrices M_{pdxB} and M_{pdxA} have the dimensions (M_{pdxB} (49·9)), respectively (M_{pdxA} (14·9)). To start the numerical simulation, the initial conditions of the elements of the two M_{pdx} matrices are needed to be known or calculated. A possibility to calculate them is to use the analytical solution of the four sub-processes. After doing the calculations, we can make the matrices (M_{pdxi}) ($i \in \{A,B\}$) for the initial conditions ((M_{pdxi})$_{IC}$) that correspond to the start sequence (k-1). In order to advance from sequence (k-1) to sequence (k) we need to use the Taylor series [20]. The numerical simulation [20] is finished when $t \geq t_{f\beta}$ (final simulation time β). In all the relations from this section we consider that the integration step (Δt) has a value that is small enough, so that the numerical integration is being done correctly. For the case of blunting process composed of two sub-processes, relations (2) and (3) can be applied to obtain the process output.

IV. The Results of the Simulations

The simulation applications are developed in MATLAB environment [21]. After simulation, the comparison between the response that results through numerical integration and the analytical response of the system is made, through the calculus of the cumulated relative error in percentage [20]. All the simulations are made for the case of continuous functioning. The tuning of both controllers C_1 and C_2 is made using an adapted form of module criterion for the case when the model of the process is expressed through PDEs (for this type of processes do not exist specific tuning methods). Using the module criterion (applied for second order processes) is obtained the general form of the controller parameters, valid for both controllers:

$$K_{PR} = \frac{T_1 + T_2}{2 \cdot K_{EX} \cdot T_\Sigma}, K_{IR} = \frac{1}{2 \cdot K_{EX} \cdot T_\Sigma}, K_{PR} = \frac{T_1 \cdot T_2}{2 \cdot K_{EX} \cdot T_\Sigma},$$

where T_1 and T_2 (through singularization) are the time constants corresponding to each of the two processes. The T_1 and T_2 constants are referring to the $T_{1\gamma}$ and $T_{2\gamma}$ constants which are calculated in each of the two cases for the corresponding values of (p). Also, $T_\Sigma = T_T + T_{EE} + T_R$. The K_{EX} constant is present in all three formulae and, while changing its value, the three controller parameters are simultaneously modified. Firstly, the value of the K_{EX} is fixed for the controller from the internal loop. After that, another value of the K_{EX} constant is chosen for the controller from the external loop. The numerical simulation of the control structure is made in order to obtain the system performances. If the performances are not enclosed in the imposed limits, the value of K_{EX} associated to C_1 is decreased progressively, for each decrease the simulation of the structure being repeated and, in each case the obtained performances being evaluated. Hence, the tuning method is an iterative one. In the case when, from a simulation to the following one, the performances of the system do not have a significant improvement, the K_{EX} constant associated to C_2 is decreased as value and keeping this value constant, the iterative procedure previously presented is repeated (modifying only the parameters of C_1) until the imposed performances are obtained. In order to obtain much better performances than the imposed ones, the iterative tuning procedure can be continued, but taking into consideration the variation form and limits of the actuating signal. The

variation of the K_{EX} constants between two successive iterations, in both controller cases, has not an imposed value (being modified considering the grade of the performances improvement from an iteration to the next one). In each controller case, decreasing the value of the K_{EX} constant we can obtain a stronger control effect (action). After applying the tuning procedure, the following parameters result: $K_{PRF} = 0.0014$, $K_{IRF} = 9.35 \cdot 10^{-5}\ \text{min}^{-1}$ and $K_{DRF} = 0.0049\,\text{min}$ (for C_1), respectively $K_{PRI} = 4.887$, $K_{IRI} = 0.5313\,\text{min}^{-1}$ and $K_{DRI} = 10.7923\,\text{min}$ (for C_2).

In Fig. 9 the comparative graph between the analytical and the numerical response of the automatic control system is presented (the variation in time of the $y_F(t, p)$ signal). The reference signal's value is fixed at 7 and the disturbance signal is generated from the PDEA1's input step type signal: $u_A(t) = D_A(t) \cdot (pH_A - 7)$, where $D_A(t) = const. = 3l/s$ is the acid's flow and $pH_A = const. = 3$ is the acid's pH. This relation shows that the value of the first sub-process output signal can be modified either through the value of $D_A(t)$ or the value of pH_A. In the tank, at the initial moment, the chemical's pH is considered 7. Also this simulation is made at the overflowing point ($p = p_f$) from the second tank (the equivalent tank).

The performances imposed on the control system are: overshoot smaller in module than 7%, steady state error at position equal to 0, settling time smaller than 40min and value of the actuating signal smaller than the saturation limit (4l/s). From Fig. 9, it results that the value of the overshoot is $\sigma = -1.217\%$ (value smaller in module than 7%) and the value of the steady state error at position $a_{stp} = 0$. Considering the fact that the system "remains" in steady state regime because the response is enclosed into the stationary band of ±3% near 7 (the imposed steady state value of the output signal), the settling time value can be considered 0min ($t_r = 0\,\text{min}$).

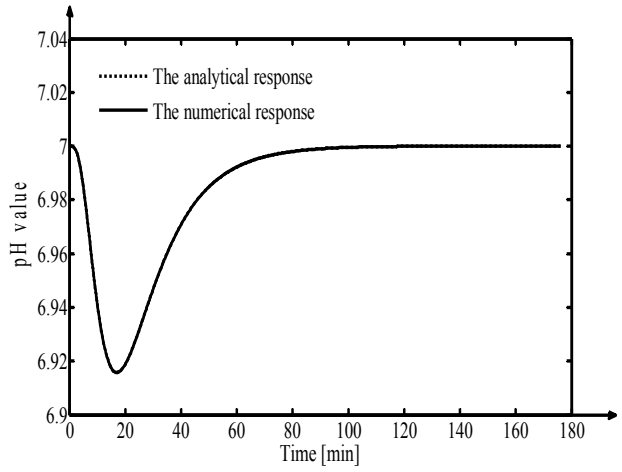

Figure 9. The comparative graph between the analytical and the numerical response of the process, at the overflowing point

On the graph we cannot differentiate the two responses due to the very small error between them. The values of the error are proportional, in steady state regime, with 10^{-3} % showing the very good performances of the numerical simulation method. The actuating signal ($f(t)$) simulated through numerical integration is presented in Fig. 10. As it can be remarked from Fig. 10, the maximum and also the steady state value of the actuating signal is 2.4 l/s, value smaller than the saturation limit.

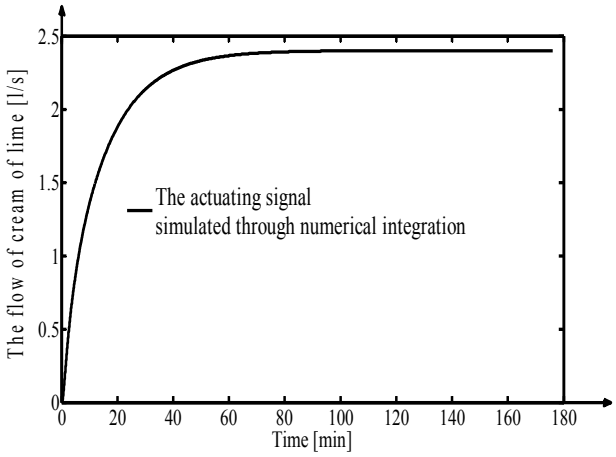

Figure 10. The actuating signal simulated through numerical integration

Another very important aspect is the fact that the actuating signal does not present value jumps.

The modeling-simulation method, being a general one, offers the user the possibility to have access to all the intermediary values. This aspect is very important in the analysis of the control system and in order to verify that the values of these variables are enclosed between the minimum-maximum limits. In all the following simulations, the false 0 value for unified current (4 mA) is considered.

In Fig. 11, the variation in time of the two measurement signals, through numerical integration, is presented.

From Fig. 11, we can remark the fact that the variation of the measurement signal is higher and faster in the case of the internal loop in comparison to the external loop case, respectively in both cases, in steady state regime, the measurement signal tends to the value 12 mA (4mA + 8mA) that corresponds to the pH value 7.

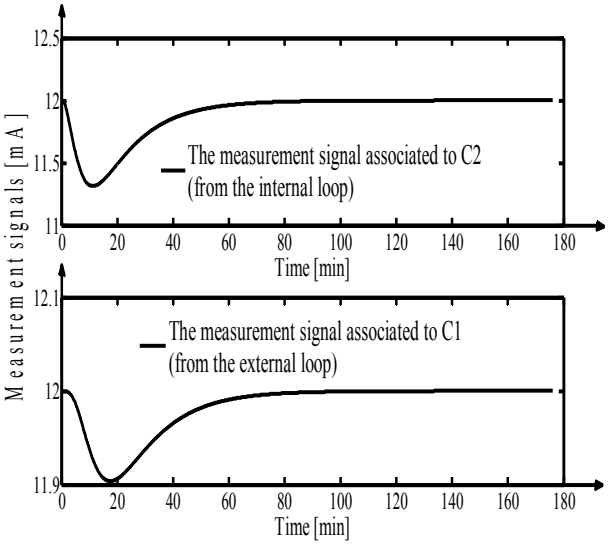

Figure 11. The two measurement signals simulated through numerical integration

In Fig. 12, the two control signals generated by the controllers C_1 and C_2, simulated through numerical integration, are presented. From Fig. 12, it results that in a

great measure, the control system forces the rejecting of the effect of the disturbance in the internal loop (the values of the control signal generated by C_2 being in each moment much higher than in the case of the control signal generated by C_1).

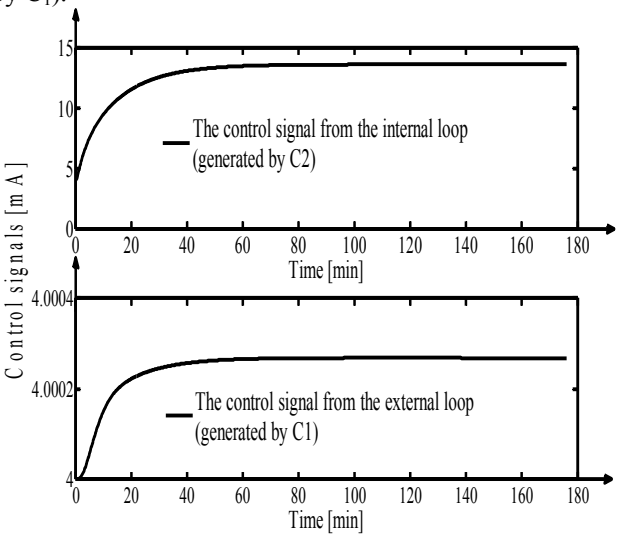

Figure 12. The two control signals simulated through numerical integration

In Fig. 13, the two error signals from the two loops, simulated through numerical integration, are presented. These two signals have, in steady state regime, the value 0mA (4mA + 0 mA) implying the fact that the main purpose of the control structure is accomplished (the value of the steady state error at the position is null).

In Fig. 14, the comparative graph between the numerical response of the automatic control system in the case of using the cascade control structure (the previous presented case) and the numerical response in the case of using a simple structure (with only one pH transducer placed at the overflowing point from the blunting system) are presented. From Fig. 14 we can notice the fact that the performances obtained in the case of using the cascade structure are much better than in the case of using the simple structure.

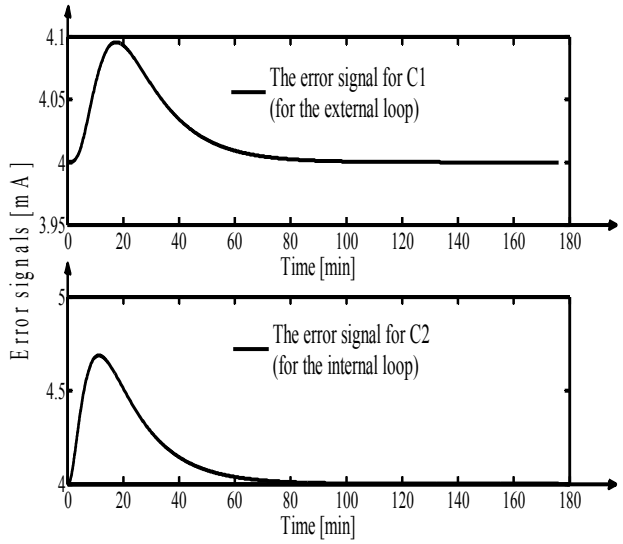

Figure 13. The two error signals simulated through numerical integration

This simulation is made for the best controller that could be obtained for the simple control structure ($K_{PR} = 8.2286$, $K_{IR} = 0.4675\,\text{min}^{-1}$ and $K_{DR} = 34.7575\,\text{min}$), the corresponding performances being $\sigma = -6.65\%$ ($|-6.65\%| \gg |-1.2\%|$), the settling time is $t_r = 64\,\text{min}$ (in the case of the cascade structure the settling time can be considered 0 min) and the value of the steady state error at position $a_{stp} = 0$ (in both cases).

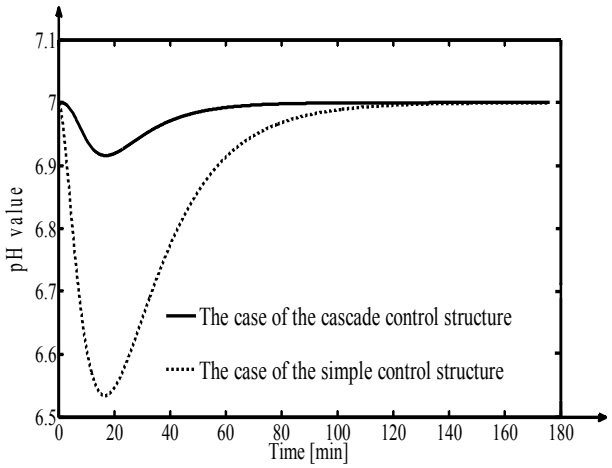

Figure 14. The comparative graph between the cases of using the cascade and the simple control structure

Also, the minimum value of the response of the simple control structure is very close to the minimum limit of 6.5, fact that has to be avoided in order to assure the safety in working.

Another important element in the problem approach is the behavior of the control system in the case of the appearance of a more restrictive disturbance. In Fig 15 is shown the comparative graph between the system's response in the initial case (case of Fig. 9; in Fig 15 with continuous line) and the system's response if $D_A(t) = const. = 4l/s$ and $pH_A = const. = 2$ (in Fig. 15 with dashed line).

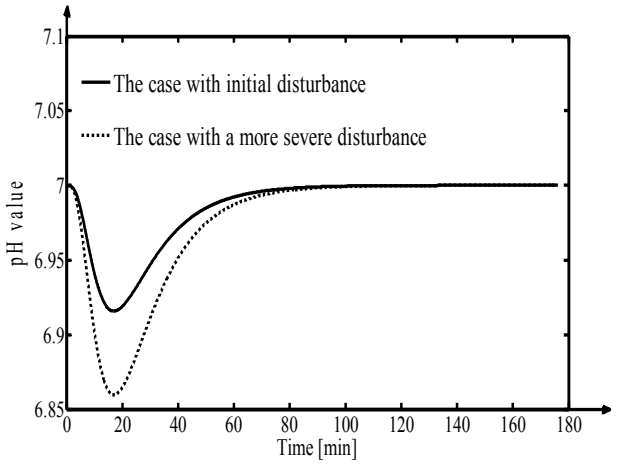

Figure 15. The comparative graph between the initial case and the case of introducing more severe disturbances

From Fig. 15 it results that the effect of the disturbance, in both cases is rejected, because in steady state regime, the value of the output signal is the imposed one (7). Also it results that, due to the higher value of the disturbance, the obtained performances (especially the overshoot) in the second case are weaker than in the initial case. The additional control effort necessary to reject the effect of the more severe disturbance obviously results from Fig. 16, the values of the actuating signal (represented with dashed line) being higher than in the initial case (with continuous line).

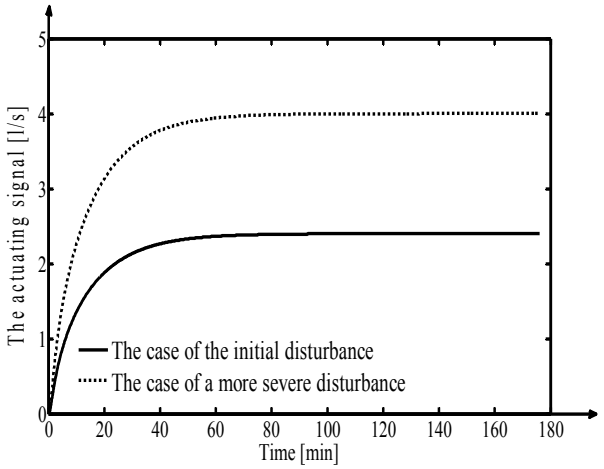

Figure 16. The comparative graph between actuating signals in the initial case and in the case of introducing more severe disturbances

Other types of possible disturbances that can appear in the system are the variable ones, for example sine type disturbances. If, over the initial disturbance from the case of Fig. 9 is superposed a sine type disturbance with the relation $u'_A(t) = 1 \cdot \sin(\omega \cdot t)$, $\omega = 0.34 rad/\min$, the comparative graph between the analytical and the numerical response of the control system is presented in Fig. 17. From Fig. 17, we can remark that the effect of the disturbance is rejected due to the fact that the system's response is enclosed in the stationary band of ±3% near 7. In this case, the value of the corresponding actuating signal, in steady state regime, varies after a sine curve near the value of 2.4 l/s.

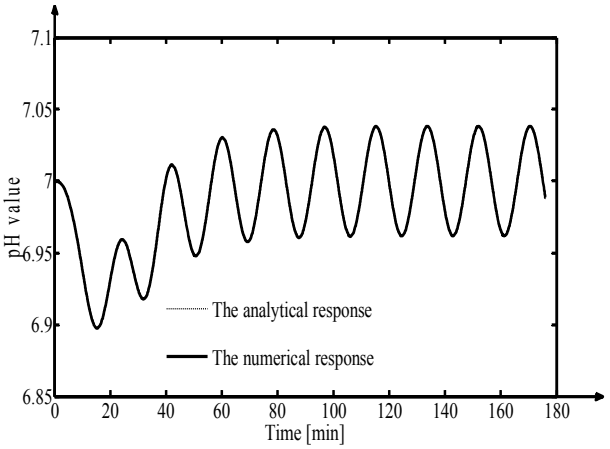

Figure 17. The comparative graph between the analytical and the numerical response of the system, if a combined step+sine type disturbance appears

V. CONCLUSIONS

The paper proposes a cascade control strategy for the pH control in a residual water blunting system. The modeling-simulation method used for the presented control system, is based on the (M_{pdx}), associated with Taylor series, method that assures a very high accuracy of the numerical simulation. The high accuracy is proved by the fact that the cumulative relative error in percentage calculated between the analytical and the numerical response of the process has very small values (near to 0). The error was presented only for the simulation from Fig. 9, but the obtained errors from all the simulations have approximately the same values as in the mentioned case. The value of the integration step that is used is $\Delta t = 0.01 \min$.

The two sub-processes from the structure of the treated process are viewed as processes with distributed parameters and are modeled through PDEs. This approach permits the pH control in different points on the tanks lengths. Although the input signals in the sub-processes are multiplication results between the reactants flows, respectively the reactants pH, we use the simplifier hypothesis that these do not introduce non-linearity [22] in their models, due to the big volume of the tanks. All the imposed performances on the control system are respected. Also, in the simulation from Fig. 14 it is shown the fact that the cascade control structure generates very good results comparing with the simple control structure, its implementation being justified.

REFERENCES

[1] V. Mureşan, M. Abrudean, M.-L. Ungureşan, T. Coloşi, "Control of the Blunting Process of the Residual Water from a Foundry," Proc. of 2012 IEEE SACI 7th edition, Timisoara, Romania, 2012.
[2] V. Mureşan, M. Abrudean, "Temperature Modelling and Simulation in the Furnace with Rotary Hearth," Proc. of 2010 IEEE AQTR 2010–17th edition, Cluj-Napoca, Romania, 2010, pp. 147-152.
[3] H.-X. Li, C. Qi. Spatio-Temporal Modeling of Nonlinear Distributed Parameter Systems: A Time/Space Separation Based Approach, 1st Edition. Springer, pp. 10-32, 2011.
[4] M. Krstic, "Systematization of approaches to adaptive boundary control of PDEs," International Journal of Robust and Nonlinear Control, vol. 16, pp. 801-818, 2006.
[5] R. F. Curtain, K.A. Morris, "Transfer Functions of Distributed Parameter Systems," Automatica, vol. 45, no. 5, pp. 1101-1116, 2009.
[6] H. Lin, P. J. Antsaklis, "Switching Stabilizability for Continuous-time Uncertain Switched Linear Systems," IEEE Transactions on Automatic Control, vol. 52, no. 4, pp. 633-646, 2007.
[7] A. Smyshlyaev, M. Krstic, "Control design for PDEs with space-dependent diffusivity and time-dependent reactivity," Automatica, vol. 41, pp. 1601-1608, 2005.
[8] P. Frihauf, M. Krstic, "Leader-enabled deployment into planar curves: A PDE-based approach," IEEE Transactions on Automatic Control, vol. 56, pp. 1791-1806, 2011.
[9] D. L. Russell, "Observability of Linear Distributed Parameter Systems," The Control Handbook, Control System Advanced Methods, William Levine, CRC Press U.S.A., pp. 70-1-70-12, 2010.
[10] I. Inoan, "Movement control of an unloading machine from a rotary furnace," Proc. of AQTR 2010, THETA 17th edition, Cluj-Napoca, Romania, 2010, pp. 131-134.
[11] I.-V. Sita, "Building Control, Monitoring, Safety and Security using Collaborative Systems," 4th Int. Conf. on Intelligent Networking and Collaborative Systems, Bucharest, Romania, 2012, pp. 662-667.
[12] R. Miron, T. Letia, "Fuzzy Logic Decision in Partial Fingerprint Recognition," AQTR 2010-THETA 17th edition, Cluj-Napoca, Romania, 2010, pp. 439-444.
[13] M. Abrudean. Systems theory and automatic regulation. Mediamira, Cluj-Napoca, pp. 78-93, 1998.
[14] A. G. Gheorghe, C. V. Marin, F. Constantinescu, M. Niţescu, "Parameter Identification for a New Circuit Model Aimed to Predict Body Water Volume," Advances in Electrical and Computer Engineering Journal, vol. 12, no. 4, pp. 83 – 86, 2012.
[15] St. Preitl, R.E. Precup, Z. Preitl. Structures and algorithms in automatic control of the processes Vol. 2. Orizonturi Universitare, Timişoara, pp. 41-62, 2009.
[16] J. Love, Process Automation Handbook. Springer, pp. 250-272, 2007.
[17] M. Vînătoru. Industrial plant automatic control, Vol. 1. Universitaria Craiova, pp. 67-80, 2001.
[18] F. Golnaraghi, B. C. Kuo. Automatic Control Systems. Wiley, pp. 487-510, 2009.
[19] F. Aghili, "Control of Brushless DC Motors," The Control Handbook, Second Edition: Control System Applications, W. S. Levine, CRC Press, pp. 23.1-23.20, 2010.
[20] T. Coloşi, M. Abrudean, M.-L. Ungureşan, V. Mureşan. Numerical Simulation of Distributed Parameter Processes. Springer, pp.264-280, 2013.
[21] User Guide, Matlab 7.5.0 (R2007b).
[22] S. Godasia, A. Karakasb, A. Palazoglu, "Control of nonlinear distributed parameter processes using symmetry groups and invariance conditions," Computers & Chemical Engineering, vol. 26, no. 7-8, pp. 1023-1036, 2002.